Preprints of the 19th World Congress
The International Federation of Automatic Control
Cape Town, South Africa. August 24-29, 2014

Fault Isolation for Urban Railway Vehicle Suspension Systems ⋆

Xiukun Wei [*,**] **Limin Jia** [*] **Kun Guo** [**] **Sheng Wu** [***]

[*] *State Key Lab of Rail Traffic Control and Safety, Beijing Jiaotong University, Beijing, 100044*
[**] *School of Traffic and Transportation,Beijing Jiaotong University, Beijing, 100044*
[***] *School of Automation, Beijing University of Science and Technology, Beijing, 100083*

Abstract: Reliability of the railway vehicle suspension system is of critical importance to the safety of the vehicle. It is very desirable to monitor the health condition and the performance degradation for rail vehicle suspension systems online, which offers the important information of the suspension system and it is critically important for the condition based maintenance rather than scheduled maintenance in the future. Advanced fault diagnosis method is one of the most effective means for the health monitoring of rail suspension systems. In this paper, taking the lateral suspension system as an example, the fault isolation issue for different component faults occurring in the suspension system is concerned. The sensor configuration for obtaining the state information for fault diagnosis and the mathematical model for the lateral suspension system are presented. Three different methods, Dempster-Shafer (D-S) evidence theory, Fisher Discrimination Analysis (FDA) and Support Vector Machine (SVM) techniques are applied to the fault isolation problem, respectively. Simulation study is carried out by means of the professional multi-body simulation tool, SIMPACK. The simulation results show that these methods can isolate the considered component faults effectively with a high accuracy. The proposed methods provide an effective alternative for the health monitoring of rail vehicle suspension systems.

Keywords: Vehicle Suspension System, Fault Isolation, D-S Evidence Theory, SVM, FDA.

1. INTRODUCTION

The suspension system is used to support the carbody and bogie, to isolate the forces generated by the track unevenness at the wheels, and to control the altitude of the carbody with respect to the track surface for providing ride comfort. For the case of urban railway, the performance of some components, such as the springs and the dampers, degrade significantly after one or two years. So it is necessary to timely detect the fault and monitor the performance degradation of vehicle suspension systems.

The health condition monitoring and fault diagnosis issue of the rail vehicle suspension systems have been paid some attention. In Bruni et al. (2007), some available health monitoring techniques are reviewed and it points out that the condition monitoring methods for railway suspension systems are critically important in the future. In Li and Goodall (2004), the fault detection issue of railway vehicle lateral suspension system is investigated, where a Kalman filter based method has been proposed for detecting and isolating faults. In Mei and Ding (2009), the authors proposed a novel approach which exploits the dynamical interactions between different vehicle modes caused by component failures in the system. In Wei et al. (2011a) and Wei et al. (2011b), a fault detection approach for the light rail vehicle suspension systems based on Kalman filter is derived. In our recent work Wei et al. (2013), different fault detection methods based on the acceleration methods for the suspension system are investigated and compared carefully. It shows that the data driven methods have more advantages than the model based methods. The current reported methods for health monitoring of rail suspension systems are mainly the fault detection methods. How to isolate the occurring faults is not investigated in the available literature. Due to the complexity of the rail suspension system, only detecting the fault is not good enough for the condition based maintenance. Finding out the concrete faulty component or isolating different faults are very desirable. These motivate the work of this paper.

This paper is organized as follows. The urban rail vehicle lateral suspension system, its state space dynamical model and the sensor configuration for obtaining the state information are introduced in Section 2. In Section 3, the fault isolation results based on Dempster-Shafer (D-S) evidence theory, the Fisher Discrimination Analysis (FDA) and the Support Vector Machine (SVM) methods are presented. Finally, some conclusions are given in Section 4.

⋆ This work is partly supported by State Key Laboratory of Rail Traffic Control and Safety (Contract No.RCS2014ZT03) and Ph.D. Programs Foundation of Ministry of Education of China (Grant number: 20110009120037).

2. THE RAIL VEHICLE LATERAL SUSPENSION SYSTEM MODELING AND SENSOR CONFIGURATION

For a rail vehicle suspension system, vertical suspension system and lateral suspension system are conventionally considered separately when the vehicle dynamics is studied. In this paper, the lateral suspension system is taken as an example to demonstrate the proposed fault isolation approach. These methods can be extended to the vertical suspension case easily.In this section, the state space dynamical model of rail vehicle suspension system is presented briefly. After that, the acceleration sensor configuration is introduced and the new state space model under the new sensor configuration is provided.

2.1 The state space model of the vehicle lateral dynamics system

The rail vehicle lateral suspension system considered in this paper is shown in Fig. 1 and Fig. 2. The suspension system connects the carbodys, the front bogie, the rear bogie and the wheelsets together. For the considered lateral suspension system, a model with 17 degrees-of-freedom (DOF) is needed for describing the dynamical behavior. The degrees-of-freedom of vehicle system's carbody, bogies and wheelsets are presented in Table 1. Standard dynamic equations for three degrees-of-freedom (DOF) (transverse, yaw and roll) carbody and bogie can refer to our former work Wei et al. (2013).

Table 1. DOF of the vehicle lateral suspension system

DOF	transverse move	yaw	roll
carbody	y	ψ	θ
front and rear bogie	y_{FB}, y_{RB}	ψ_{FB}, ψ_{RB}	θ_{FB}, θ_{RB}
1,2,3,4 wheelset	y_{W1}, y_{W2}, y_{W3}, y_{W4}	ψ_{W1}, ψ_{W2}, ψ_{W3}, ψ_{W4}	

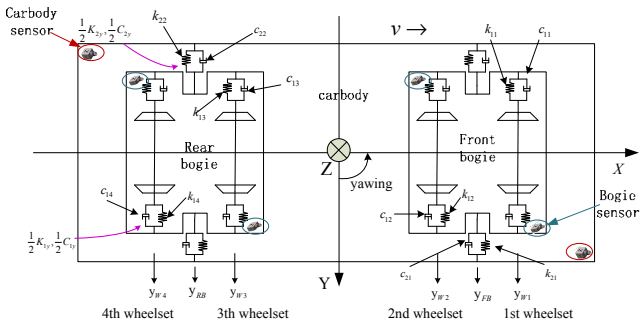

Fig. 1. Top view of the vehicle's lateral dynamical model

In the light of the differential equations, the state space equation of the lateral suspension system is as follows:

$$\dot{x}_v = A_v x_v + B_v d \tag{1}$$

$$y_v = C_v x_v + D_v d \tag{2}$$

where

$$x_v = [\dot{y} \quad \dot{\psi} \quad \dot{\theta} \quad y \quad \psi \quad \theta \quad \dot{y}_{FB} \quad \dot{\psi}_{FB} \quad \dot{\theta}_{FB}$$
$$y_{FB} \quad \psi_{FB} \quad \theta_{FB} \quad \dot{y}_{RB} \quad \dot{\psi}_{RB} \quad \dot{\theta}_{RB} \quad y_{FB} \quad \psi_{FB} \quad \theta_{FB}$$
$$\dot{y}_{W1} \quad \dot{\psi}_{W1} \quad y_{W1} \quad \psi_{W1} \quad \dot{y}_{W2} \quad \dot{\psi}_{W2} \quad y_{W2} \quad \psi_{W2} \quad \dot{y}_{W2}$$
$$\dot{\psi}_{W3} \quad y_{W3} \quad \psi_{W3} \quad \dot{y}_{W4} \quad \dot{\psi}_{W4} \quad y_{W4} \quad \psi_{W4}]^T$$

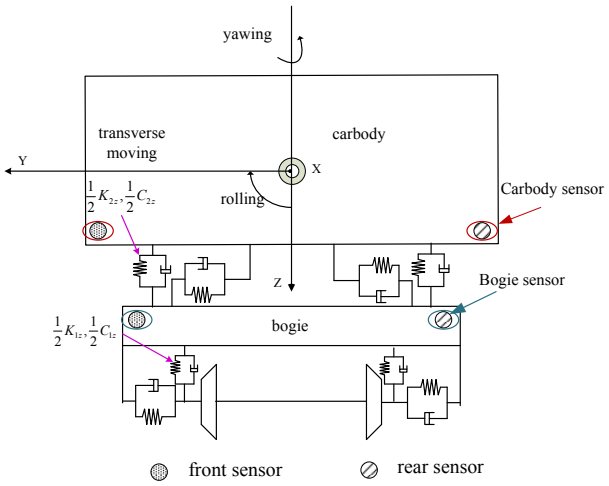

Fig. 2. Front view of the vehicle's lateral dynamical model

$$d = [\, y_{t1} \;\; y_{t2} \;\; y_{t3} \;\; y_{t4} \,]^T$$
$$y_v = [y \;\; \psi \;\; \theta \;\; y_{FB} \;\; \psi_{FB} \;\; \theta_{FB} \;\; y_{RB} \;\; \psi_{RB} \;\; \theta_{RB}]^T$$

The matrix A_v, B_v, C_v and D_v are derived from the differential equations presented before. d is the track lateral irregularity.

2.2 The sensor configuration for the signal measurements

In the model derived in the last subsection, the placement, the yaw angle and the pitch angle of the carbody, the front and rear bogie are taken as the outputs. The system is detectable and observable in the course of the system theory. This means that the changes of the system states can be observed by the outputs in a limited time range. When component faults occur in the system, they can be detected by the outputs. However, in reality, the placements for the carbody, the front and rear bogie are difficult to measure and few ideal and reliable sensors can be applied to measure these placements. Similarly, effective and high precision roll and yaw angle sensors for the concerned problem are not available as for the knowledge of the authors. These comments are also stated in our former work Wei et al. (2013).In this paper, a new sensor configuration is also proposed to the fault isolation problem for the lateral suspension system. The vehicle suspension system is only equipped with acceleration sensors on two of the four corners of the carbody, the front and rear bogie. Each sensor can measure the vertical acceleration and lateral acceleration simultaneously. Carbody sensors are equipped in two diagonal corners on the floorboard. The two bogie sensors are equipped in the sides faced to outside and one is in the front and the other is in the rear(see Fig. 1 and Fig. 2). The acceleration signal can be transformed to displacement signal by applying double integral to the acceleration signal, that is

$$y = \iint a dt dt \tag{3}$$

where a is the acceleration value and y is the transverse displacement.

Remark 1. In principle, the displacement signal can be obtained by double integrating the acceleration signal directly. However, in reality, the output of acceleration sensors always contains DC component. The DC component

must be filtered by a high pass filter. The numerical integral algorithm is also critical to achieve a high accuracy.

3. FAULT ISOLATION SIMULATION

In this paper, the data acquired from the vehicle suspension system are preprocessed (such as DC filtering, double integrating) before the statistical fault features are calculated. The obtained fault features are extracted by principle component analysis technique. After that, the pattern classification, such as the SVM, FDA methods, and the D-S evidence theory are applied to the fault class identification.

3.1 Simpack vehicle modeling and suspension system fault simulation

To analyze and study the fault isolation performance of the three methods, a SIMPACK and MATLAB co-simulation environment is built. The parameters are provided by the vehicle manufacturer to obtain the simulation data for the purpose of algorithm validation. The multi-body simulation model is built by the construction of coordinates system, bodies, joints, constraints, force elements, track excitations and so on. The SIMPACK vehicle model is used to generate the acceleration signals and to simulate different faults in both primary and secondary suspensions. The SIMPACK vehicle suspension simulation model equipped with acceleration sensors is shown on the right part of Fig. 3. The track irregularity used in the simulations is the fifth-grade track irregularity spectrum of the US railway lines. The proposed sensor configuration is seen in Fig. 1. Furthermore, it should be stated here that the fault detection results do not depend on the special track irregularity.

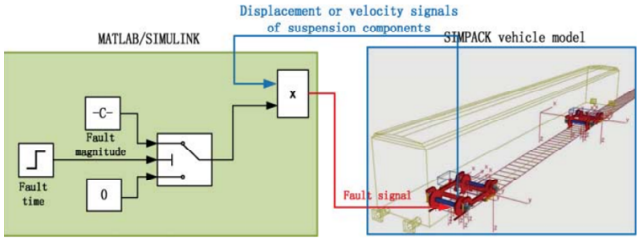

Fig. 3. The vehicle suspension fault simulation based on Matlab-SIMPACK software

In this paper, by using the interface between SIMPACK and MATLAB, construct urban rail vehicle suspension system fault simulation experiment model as shown in Fig. 3, to realize the vehicle component faults simulation of suspension system at an arbitrary time instant and with an arbitrary amplitude. The principle of the fault simulation is described as follows:

Take the fault of damper as an example. In the light of the working principle of the damper component, the force generated by the damper is equal to the damper coefficient times piston's velocity, which is used to prevent the moving of the piston. The force is proportional to the velocity of movement of the piston, the direction is opposite to the movement of the piston. It can be stated as:

$$F_C = C \cdot v \tag{4}$$

where, C is the damping coefficient, v is the velocity of the piston. When the damper is faulty and its performance degrades, for instance, the coefficient has a 25% reduction, a smaller force is generated by the damper and the reduced force is proportional to the product of the piston's velocity and the reduced damper coefficient. To simulate the damper faulty behavior, a virtual force is generated in the light of the fault scenarios and acts on the position where the damper is fixed. As shown in Fig. 3, for instance, sensors are equipped at the position of a secondary damper to measure its moving velocity. Assume that the damper coefficient is reduced to half of its normal value at the $20th$ second (controlled by MATLAB), then an external force (the fault signal in Fig. 3) is exerted on the piston to reduce the resistance generated by the damper. The direction of the virtual force is opposite to the force generated by the damper and the value of force is equal to the fault magnitude times the piston's velocity. The effective force is described as follows when the damper occurs a failure:

$$F_C = C \cdot v - C_{re} \cdot v \tag{5}$$

where, C_{re} denotes the damping coefficient attenuation values of the faulty dampers.

In a similar way, spring failure can also use a similar method to simulate. In the course of simulation, MATLAB needs to get the signal of the displacements of the faulty spring location in which the fault occurs. The effective force is described as follows when the spring occurs a failure:

$$F_K = K \cdot s - K_{re} \cdot s \tag{6}$$

where, K denotes the spring stiffness in normal condition, K_{re} denotes the attenuation value of stiffness coefficient.

3.2 Spring and damper faults of the suspension system

In this paper, the vehicle lateral suspension system is taken as an example for the presented fault isolation methods. The considered suspension component faults are mainly the primary spring stiffness faults, the secondary spring stiffness faults and the secondary damping coefficient loss faults. For each component, both the middle level fault (MF) and the severe fault (SF) are considered in the fault isolation issue. In total, 16 different faults are used in the fault isolation simulation study. The detailed faults description considered in this paper are described in Table 2 and the concrete occurring location for the considered faults is shown in Fig. 1.

3.3 MF and SF used for the fault isolation

The faults of the springs and the dampers can be indicated by the changes of the spring stiffness or the damping coefficient. In the light of the range of the coefficients, the faults can be divided into different types, for instance, small level faults, middle level faults and severe level faults. A small level fault of a component means that its stiffness reduction or damping coefficient loss is in the range between 0% and 25%. The middle level fault(MF) has coefficient change in the range between 26% and 60%. The coefficient change of the severe level fault(SF) is greater than 60%. In our former work Wei et al. (2013), the

Table 2. Spring and damper faults of the vehicle lateral suspension system

Fault No.	Fault Component	Fault Type	Fault Description
1	c_{21}	MF	26% ∼ 60% damping reduction
2	c_{21}	SF	60% ∼ 100% damping reduction
3	k_{21}	MF	26% ∼ 60% stiffness reduction
4	k_{21}	SF	60% ∼ 100% stiffness reduction
5	c_{22}	MF	26% ∼ 60% damping reduction
6	c_{22}	SF	60% ∼ 100% damping reduction
7	k_{22}	MF	26% ∼ 60% stiffness reduction
8	k_{22}	SF	60% ∼ 100% stiffness reduction
9	k_{11}	MF	26% ∼ 60% stiffness reduction
10	k_{11}	SF	60% ∼ 100% stiffness reduction
11	k_{12}	MF	26% ∼ 60% stiffness reduction
12	k_{12}	SF	60% ∼ 100% stiffness reduction
13	k_{13}	MF	26% ∼ 60% stiffness reduction
14	k_{13}	SF	60% ∼ 100% stiffness reduction
15	k_{14}	MF	26% ∼ 60% stiffness reduction
16	k_{14}	SF	60% ∼ 100% stiffness reduction

fault detection issue for the rail vehicle suspension system is investigated. It shows that for most of the component faults, the small fault (coefficient loss less than 25%) is difficult to be detected. Hence, the fault isolation issue for small faults is not considered in this paper. Only the middle level faults and severe faults isolation issue are concerned in the following. A typical presentive value for the middle level fault is 50% stiffness or damping coefficient loss and the value for the severe fault is 75%. The aim of the fault isolation of this paper is two folds. On the one hand, the fault isolation method can identify which component occurs a fault. On the other hand, the occurred fault is a middle level fault or a severe level fault. The performance is evaluated by the fault component identification accuracy(FCA) and the faulty type prediction accuracy(FTA) defined in the following respectively.

$$FCA = \frac{\text{Number of correctly predicted component}}{\text{Number of total component fault}} \times 100\%$$

$$FTA = \frac{\text{Number of correctly predicted type}}{\text{Number of total component fault type}} \times 100\%$$

3.4 Data acquisition and fault feature calculation

The total simulation time is 50s and all the different faults occur at 20s after the simulation starts. The 12 acceleration signals at the bogie corners and carbody corners are recorded with a sampling time 0.1s. By using double integration, the displacement signals of the bogie and carbody corners are obtained. For each considered fault with a specified fault magnitude, the measurements in 50s are recorded with a length of 500 time instants.

For each recorded measurement, the seven fault features (4 in the time domain and 3 in the frequency domain) are calculated. Since we have 12 sensors for 12 displacement signals, 84 fault feature values are obtained for a component fault with specified magnitude.

Due to the existence of irrelevant and useless features in the 84 features, it is helpful for the fault isolation performance by using principal component analysis(PCA) to reduce the fault feature dimension and extract the principal fault features.

3.5 Case study based on D-S evidence theory

In this section, the application of the D-S evidence theory to the fault isolation is presented. The considered new occurred fault types are the same with the recorded faults in the database Table 2, while the fault magnitudes are different from the fault magnitudes recorded in the fault database, which are 50% for middle level fault (MF) and 75% for severe level fault (SF).

The fault isolation results based on the D-S evidence theory for the secondary spring k_{21} with a fault magnitude 50%(MF) and a primary spring k_{13} with a fault magnitude 75%(SF) are shown in Fig. 4 and Fig. 5, respectively. Where, the maximum of vertical coordinate corresponding to lateral coordinate is the most likely occurring fault.

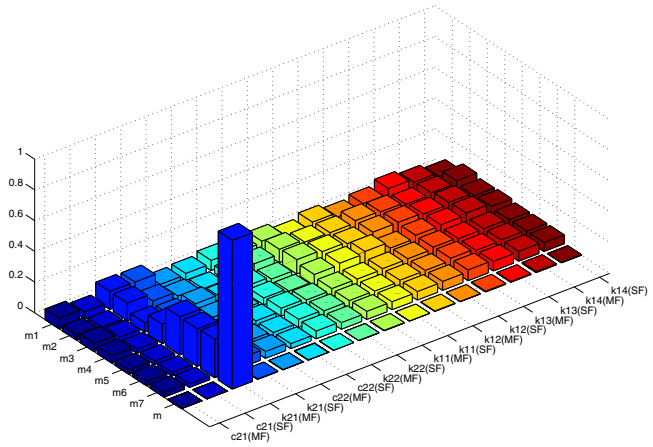

Fig. 4. Simulation case of k_{21}_50%

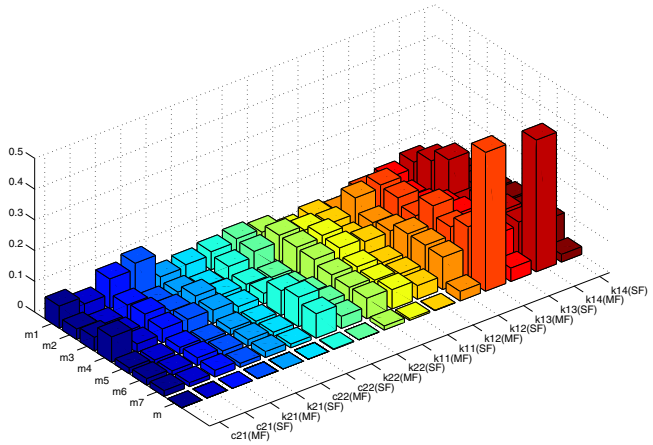

Fig. 5. Simulation case of k_{13}_75%

As shown in Fig. 4, the first line m_1 , is the normalized distance similarity between the first feature of the new occurred fault and all recorded faults in the database. In the same way, the other lines $m_2, \cdots, m_7$, are the other six pieces of normalized distance similarity for other six features respectively. In terms of the principles of decision making, the decision about the isolation result is made. $k_{21}(MF)$ is the maximum of the BBAs, and it is lager than the other BBAs. From this result, $k_{21}$is considered as

the most possible occurred fault. Furthermore, this fault magnitude of obtained result is predicted in MF correctly. The final result is consistent with the new occurred fault.

In the same way, the result of Fig. 5, depicts that the fault component can be predicted correctly. However, the fault type is isolated wrongly.

In summary, at the first, from the isolation results, primary spring can be clearly distinguished with secondary spring and damper; Secondly, all the faulty components are predicted correctly. However, two primary spring faulty types are not predicted correctly. Hence, the FCA is 100% for the D-S evidence theory based fault isolation method. Its FTA is 83.3%.

3.6 SVM fault isolation results

The SVMs-based multi-class classification is applied to perform the fault isolation process of the suspension system. Three different fault magnitudes (for instance, 45%, 47% and 53% for middle level fault and 70%, 72% and 78% for severe fault) are recorded for each component fault. The fault features are calculated and extracted by using PCA, respectively. Theses fault features are used for the SVM classifier training by using different kernel functions. To validate the fault isolation effectiveness, new component fault with different fault magnitudes used in the training fault set (for instance, 50% for middle level fault and 75% for severe fault) is generated. Similarly, the fault features are calculated and extracted by using PCA, respectively. The LIBSVM toolbox is applied to the SVM training and prediction. The suspension fault isolation results are shown in Table 3 and Table 4.

Table 3. Fault isolation results using original feature and SVM

Kernel	FCA (%) Training	FCA (%) Testing	FTA (%) Training	FTA (%) Testing
Linear	100	68.75	100	68.75
Polynomial (d=1,$\gamma = 0.1$)	100	75	100	68.75
Gassian RBF (C=100, $\gamma = 0.0001$)	100	75	100	68.75

Table 4. Fault isolation results using PCA feature extraction and SVM

Kernel	FCA (%) Training	FCA (%) Testing	FTA (%) Training	FTA (%) Testing
Linear	100	68.75	100	68.75
Polynomial ($d = 1, \gamma = 0.1$)	100	75	100	68.75
Gassian RBF ($C = 100$, $\gamma = 0.0001$)	100	87.5	100	75

From the fault isolation simulation results, it can be seen that the SVM with Gassian RBF kernel receives the best performance as it is expected. The training data achieves a 100% accuracy with all the methods. However, there are some wrong predictions when using the testing data. It is observed that all the secondary spring and damper faults (both faulty component and faulty type) are isolated correctly. However, two primary spring faulty components are not predicted correctly. Four primary spring faulty types are predicted wrongly.

Remark 2. Due to the complexity and nonlinearity of the lateral suspension system, it is difficult to isolate all the component faults with 100% accuracy rate. However, the training data achieves a perfect isolation result. Note that the occurring fault is in the training fault set, the faulty component and also its faulty type can always be predicted correctly. Hence, a training fault set with enough different fault magnitudes is very helpful for real application.

3.7 FDA fault isolation results

In this section, the Fisher Discrimination Analysis is applied to the fault isolation issue. The data used to obtaining the Fisher discriminant projection vectors are the same to the one used in the SVM fault isolation method. The testing fault set is also the same as used before. The Mahalanobis distance method is used for classifying the fault.

It is observed that the FDA method can achieve 100% FTA and FCA accuracy rates when the training fault set is used to classify. For the testing fault set, the calculated Mahalanobis distances for each testing fault to the fault class are shown in Table 5. The smallest distance are bold-faced. It can be seen that 3 faults in the 16 faults are isolated into wrong fault types. Hence, the FTA rate is 81.25%. The fault $k_{11}(SF)$ is classified into $k_{11}(MF)$. However, the fault component is still correctly identified as k_{11}. The FDA method also achieves a high FCA rate as 87.5% for the testing faults.

3.8 Comparison of the three fault isolation methods

From the fault isolation results of the three methods, it is shown that D-S evidence theory achieves the best fault component isolation accuracy (100%). It means that all the faulty components are correctly identified. In the mean time, the FTA of D-S evidence theory is also higher than that of the other two methods (FDA and SVM). Furthermore, the D-S evidence theory is also robust to the fault magnitudes. FDA achieves a little better performance than SVM method combined with PCA technique. However, the algorithm of FDA is simpler and easier to be implemented than SVM method which need a multi-objective optimization solver.

4. CONCLUSIONS

In this paper, using the lateral rail vehicle suspension system as an example, the fault isolation issue for the different component faults occurring in the suspension system is concerned. The mathematical model for the lateral suspension system is presented. The acceleration sensor configuration for obtaining the state information is introduced. After that, three different methods, Dempster-Shafer (D-S) evidence theory, Fisher Discrimination Analysis (FDA) and Support Vector Machine (SVM) techniques are applied to the fault isolation problem, respectively. Simulation study is carried out by means of the multi-body simulation tool, SIMPACK. The simulation results show that these methods can isolate the considered

Table 5. Mahalanobis distances of the testing faults to the fault class. Smallest is Bold-faced

Fault No.	c_{21} (MF)	c_{21} (SF)	k_{21} (MF)	k_{21} (SF)	c_{22} (MF)	c_{22} (SF)	k_{22} (MF)	k_{22} (SF)
1	**0.0076**	0.1038	1.1035	0.1464	**0.1969**	0.1216	0.4793	1.1988
2	0.0277	**0.0120**	0.3670	0.1253	1.2455	0.4305	0.4099	1.2307
3	0.0740	0.3518	**0.0139**	0.1334	0.4860	0.1206	1.1106	0.5598
4	0.0580	0.0510	0.0752	**0.0180**	0.5358	1.2640	2.0196	0.7620
5	0.0247	0.5465	3.7952	0.0749	0.6357	0.2040	3.8190	0.5271
6	0.0103	0.4798	0.2915	0.0877	1.1210	**0.0136**	0.4964	0.5263
7	0.0380	0.3797	1.8689	0.1263	0.3739	0.2689	**0.0360**	0.4070
8	0.1186	1.2395	0.1927	0.0477	2.0352	0.4136	1.6476	**0.0926**
9	0.2572	0.0549	0.5249	0.4330	0.8748	0.1803	0.1849	0.3375
10	0.2235	0.6657	0.2182	0.0240	5.0460	0.1067	0.1629	1.8042
11	0.0738	0.2540	3.4569	0.2780	0.5830	0.2471	0.4489	1.0122
12	0.0364	0.3423	0.7274	0.0395	2.5316	0.7984	0.1485	1.4688
13	0.8066	0.0348	0.9331	0.0475	1.0377	0.0302	2.4915	5.9040
14	0.6270	1.2240	0.3235	0.2135	1.1089	2.3689	0.9140	0.5937
15	1.1002	0.7852	0.7810	0.1517	2.7122	1.9658	0.7907	1.3779
16	0.0446	0.2697	1.4075	0.1170	3.3318	1.0879	0.5195	1.7295

Fault No.	k_{11} (MF)	k_{11} (SF)	k_{12} (MF)	k_{12} (SF)	k_{13} (MF)	k_{13} (SF)	k_{14} (MF)	k_{14} (SF)
1	3.1386	1.1838	0.8568	0.5311	0.5666	3.6652	0.2313	3.2469
2	4.1517	0.6024	1.4252	2.0525	0.5525	1.6277	0.8471	4.2705
3	6.0041	1.5981	0.4230	3.6004	1.3566	4.0655	2.7858	2.0654
4	2.4287	0.2171	0.4578	**0.0270**	0.4041	1.4931	0.8965	1.8868
5	2.4240	0.8532	1.1239	7.0076	0.0958	2.9378	0.5044	7.3589
6	3.8151	0.1233	0.2636	0.1657	0.3778	2.1067	1.2011	0.2736
7	1.3116	0.2960	0.2483	0.5591	0.1172	1.5492	0.2816	6.1455
8	0.9039	0.8944	0.3928	2.8747	0.0621	4.6444	1.1692	1.0304
9	**0.2230**	**0.1165**	0.3845	0.4196	0.0933	2.8077	0.8150	1.7349
10	0.5295	1.1994	0.0236	1.9777	0.1370	5.2057	0.0864	0.9553
11	1.3407	0.3501	**0.0087**	2.4016	0.2157	1.3455	0.0864	0.5432
12	4.9313	0.7712	0.5286	0.8107	0.8082	0.9412	1.1583	7.8229
13	0.7651	0.3364	0.1454	2.4230	**0.0192**	1.7997	0.7187	2.1729
14	1.1430	2.0749	3.1263	0.8474	0.1067	**0.2002**	0.4456	6.5478
15	1.4894	1.2324	0.6056	4.1263	0.1047	1.8135	**0.0597**	0.4216
16	0.5532	0.2428	1.6628	3.3961	0.1897	3.7896	0.3834	**0.2508**

component faults effectively with a high accuracy. In these three methods, the isolation accuracy rate of FDA and SVM techniques depend on the training fault set. However, the D-S evidence method is robust to the fault magnitude changes. The proposed method provides an effective alternative for the health monitoring of rail vehicle suspension systems.

In this paper, the lateral suspension system is taken as a example for the considered urban rail vehicles. However, the sensor configuration, modeling and the fault isolation methods can be trivially extended to the vertical suspension system. Also the proposed methods can be applied to other rail vehicles, such as high speed railway vehicles. In addition, the proposed methods can also being applied to the gyro sensor configuration framework when robust and cheap gyros are available.

The fault scenarios caused in this paper are mainly one component fault occurring at a time instant. However, it is very possible that the performance of several components in the suspension system degrade simultaneously due to component aging. In addition, the disturbances caused by the tracks (for instance, the track irregularities) and the wheel defects (for instance, the wheel-flat) are not considered in our study. This will be carried out in the future work.

REFERENCES

Bruni, S., Goodall, R., Mei, T.X., and Tsunashima, H. (2007). Control and monitoring for railway vehicle dynamics. *Vehicle System Dynamics*, 45(7-8), 765–771.

Li, P. and Goodall, R. (2004). Model based condition monitoring for railway vehicle systems. In *Control 2004*, ID–508. University of Bath.

Mei, T.X. and Ding, X.J. (2009). Condition monitoring of rail vehicle suspensions based on changes in system dynamic interactions. *Vehicle System Dynamics*, 47(9), 1167–1181.

Wei, X., Jia, L., and Liu, H. (2013). A comparative study on fault detection methods of rail vehicle suspension systems based on acceleration measurements. *Vehicle System Dynamics*, 51(5), 700–720.

Wei, X., liu, H., and Qin, Y. (2011a). Fault diagnosis of rail vehicle suspension systems by using GLRT. In *Chinese Control and Decision Conference*, 1932–1937. Mianyang, China.

Wei, X., Liu, H., and Qin, Y. (2011b). Fault isolation of rail vehicle suspension systems by using similarity measure. In *International Conference on Intelligent Railway Tranportation*, 391–396. Bei Jing, China.